https://doi.org/10.5194/acp-2020-806
Preprint. Discussion started: 31 August 2020

Atmospheric Chemistry and Physics Discussions

Aqueous phase oxidation of bisulfite influenced by nitrate photolysis

Lu Chen[a], Lingdong Kong[a, b,*], Songying Tong[a], Kejing Yang[a], Shengyan Jin[a], Chao Wang[a], Lin Wang[a]

[a] Department of Environmental Science & Engineering, Jiangwan Campus, Fudan University, No. 2205 Songhu Road, Shanghai, 200438, China

[b] Institute of Eco-Chongming, East China Normal University, No.3663 Northern Zhongshan Road, Shanghai 200062, China

Correspondence to: Lingdong Kong (ldkong@fudan.edu.cn)

https://doi.org/10.5194/acp-2020-806
Preprint. Discussion started: 31 August 2020

Atmospheric Chemistry and Physics Discussions

ABSTRACT: Nitrate aerosol is ubiquitous in the atmosphere, and it can exit in both solid aerosol particles and fog and cloud droplets. Nitrate in the aqueous and particulate phase can undergo photolysis to produce oxidizing active radicals, which will inevitably affect various atmospheric chemical processes. However, the role of nitrate aerosols in these atmospheric photochemical processes remains unclear. In this study, the effects of nitrate photolysis on the aqueous phase oxidation of bisulfite under different conditions were investigated. Results show that nitrate photolysis can significantly promote the oxidation of bisulfite to sulfate. It is found that pH plays a significant role in the reaction, and ammonium sulfate has significant impacts on regulating the pH of solution and the enhancement of sulfate production. We also found an apparent synergism among halogen chemistry, nitrate and its photochemistry and S(IV) aqueous oxidation, especially the oxidation of halide ions by the nitrate photolysis and by the intermediate peroxymonosulfuric acid (HSO_5^-) produced by the free radical chain oxidation of S(IV) in acidic solution leads to the coupling of the redox cycle of halogen with the oxidation of bisulfite, which promotes the continuous aqueous oxidation of bisulfite and the formation of sulfate. In addition, it is also found that O_2 is of great significance on nitrate photolysis for the conversion of HSO_3^-, and H_2O_2 generation during the nitrate photolysis is verified. These results provide a new insight into the heterogeneous aqueous phase oxidation pathways and mechanisms of SO_2 in cloud and fog droplets and haze particles.

https://doi.org/10.5194/acp-2020-806
Preprint. Discussion started: 31 August 2020

■ INTRODUCTION

The frequent haze events in China in recent years brought about severe impacts on air quality, regional and global climates and human health (Huang et al., 2014; Ji et al., 2014; Zheng et al., 2015b; Zheng et al., 2015a; Li et al., 2014). Secondary aerosols are recognized as a main cause of particulate pollution during haze events (Guo et al., 2014), of which secondary inorganic aerosols produced by the atmospheric conversions of SO_2 and NO_x under adverse meteorological conditions are the predominant components (Li et al., 2018b; Sun et al., 2014). Field measurements show that during haze episodes, most of the particles especially the sub-micrometer particles were in the aqueous state owing to the enrichment of aerosol liquid water by the elevated relative humidity (RH) and inorganic fraction in particles (Liu et al., 2017b). As a result, the occurrence of heterogeneous aqueous phase reaction has a marked tendency (Kong et al., 2018), and the role of heterogeneous aqueous phase reaction of SO_2 played in secondary sulfate aerosol formation was emphasized (Quan et al., 2015). Generally, the aqueous phase oxidation pathways of SO_2 in the cloud and fog droplets include oxidation by H_2O_2, oxidation by O_3 (Seinfeld and Pandis, 2006), and oxidation by O_2 under the catalysis of certain transition metal ions (Ibusuki and Takeuchi, 1987). At pH ~2-5, the oxidation by H_2O_2 has been considered as the dominant aqueous phase oxidation pathway for sulfate formation (Ye et al., 2018; Shen et al., 2012). This pathway includes the uptake of SO_2 (R1, see in Table 2) and subsequent aqueous phase oxidation of S(IV) (Alexander et al., 2003). In the pH range of 2-7, most of the dissolved SO_2 will be present as HSO_3^- in the solution (Hua et al., 2008), and the oxidation of S(IV) species

https://doi.org/10.5194/acp-2020-806
Preprint. Discussion started: 31 August 2020

leads to the formation of sulfate (R2). In addition, previous studies proposed that the aqueous-phase oxidation of S(IV) by NO_2 played a dominant role in sulfate production in northern China (Wang, 2016; Cheng et al., 2016), and the acid-base neutralization of NH_3 is thought to be the reason of promoting SO_2 and NO_2 to form corresponding sulfate and nitrate. However, their conclusion was doubted by Liu et al. and Guo et al. (Liu et al., 2017a; Guo et al., 2017), who found that the reaction on the actual fine particles with pH values of ~4.2 was too slow to account for sulfate formation. Therefore, some potential oxidation pathways and mechanisms for atmospheric aqueous phase oxidation of S(IV) still remain poorly understood.

Nitrate aerosol constitutes a substantial fraction of fine particles (Tao et al., 2018), and surface nitrate can change the hygroscopicity of original particles (Hoffman et al., 2004), which can be transformed into droplets at a certain RH. Field observation showed that the remarkably enhanced nitrate formation was observed during haze episodes in China (Ji et al., 2014; Tao et al., 2018), which is coincident with the high level of sulfate (Zheng et al., 2015b; Quan et al., 2015), suggesting the impact of nitrate on sulfate formation or the mutual influence between their formation processes in the atmosphere (Du et al., 2019; Kong et al., 2014). Several studies have verified that nitrate does participate in the heterogeneous conversion of SO_2. Du et al. (2019) proved that the photolysis of adsorbed nitrate can be coupled with SO_2 oxidation and sulfate formation, which is reflected in the consumption of adsorbed nitrate and the formation of adsorbed N_2O_4 during the introduction of SO_2. Kong et al. (2014) found that nitrate can accelerate the formation of sulfate on hematite and lead to the generation of surface-

https://doi.org/10.5194/acp-2020-806
Preprint. Discussion started: 31 August 2020

adsorbed HNO_3 and gas-phase N_2O and HONO under no light. And recently, Gen et al. (2019b) proposed that nitrate photolysis at 250 nm is the major source of NO_2 and •OH to oxidize dissolved SO_2, in which •OH is believed to be formed when O_2 exists, and the reaction of •OH with dissolved SO_2 generates SO_3^{2-}, which leads to the chain reaction involving SO_5^-, HSO_5^- and SO_4^- to produce multiple SO_4^{2-} from each attack of •OH on dissolved SO_2, providing a new insight for the heterogeneous aqueous phase oxidation of SO_2 by nitrate photolysis. However, the impacts of various oxidizing species produced and/or initiated by nitrate photolysis under different conditions on the aqueous phase oxidation of SO_2 remain unclear. To further reveal the aqueous phase oxidation mechanisms of SO_2 in ambient atmosphere, more potential pathways for oxidant generation and S(IV) aqueous phase oxidation, and more ambient factors such as the influence of coexisting substances, are still needed to be explored.

Halide ions (e.g. Cl^-, Br^-, I^-) are ubiquitous in the atmosphere via the transport of sea salt aerosols, the emission of fossil fuel combustion and biomass burning (Richards et al., 2011; Cahill et al., 1992; Cheng et al., 2000). The influence of halide ions on the formation of NO_2 during the photochemistry of halide-nitrate ion mixtures has been extensively studied (Richards et al., 2011; Richards and Finlayson-Pitts, 2012; Richards-Henderson et al., 2013; Wingen et al., 2008; Custard et al., 2017). For example, Wingen et al. (2008) observed enhanced NO_2 production from photolysis of deliquesced nitrate aerosols containing chloride ions, and the reason was suggested that halide ions can draw nitrate ions closer to the interface. Richards et al. (2011) found that irradiated aqueous mixtures of $NaBr/NaNO_3$ exhibit an enhancement in the rates

https://doi.org/10.5194/acp-2020-806
Preprint. Discussion started: 31 August 2020

of formation of NO_2 and Br_2 as the bromide mole fraction increased. However, up to now, little attention has been paid to the effect of chemistry of halide ions on sulfate formation under nitrate photolysis.

In this study, the aqueous phase oxidation of bisulfite influenced by nitrate chemistry was investigated under different pH and irradiation intensity. Compared to earlier works, different mechanisms for the generation of oxidants and the oxidation of S(IV) species were discussed. The pH was controlled by added ammonium sulfate and ammonium bisulfate because they coexist widely with nitrate in the atmospheric aerosol particles, in which the crucial role of NH_4^+ on sulfate formation was also highlighted. In the meantime, 2-propanol was premixed as inhibitor and •OH scavenger to examine the roles of O_2 and •OH on the aqueous phase oxidation of bisulfite. Based on this study, the formation of H_2O_2 via the recombination of •OH was verified. And furthermore, the promotion effect of the redox cycling of halogen on the aqueous phase oxidation of bisulfite under nitrate photolysis was investigated.

■ MATERIALS AND METHODS

Materials. Aqueous stock solutions of sodium bisulfite (ACS reagent, Sigma-Aldrich), ammonium nitrate, ammonium sulfate (≥99.99% metals basis, Aladdin), ammonium bisulfate (≥99.99% metals basis, Aladdin), sodium chloride (analytical reagent, Shanghai Qiangshun Chemical Reagent Co., Ltd.), sodium bromide (≥99.99% metals basis, Aladdin) and sodium iodide (≥99.99% metals basis, Aladdin) were prepared by dissolving the corresponding salt in Milli-Q water. 2-propanol (HPLC Plus)

https://doi.org/10.5194/acp-2020-806
Preprint. Discussion started: 31 August 2020

was purchased from Sigma-Aldrich. All the chemicals were used without further purification.

Photochemical Experiments. Experiments were conducted in a cylindrical quartz glass cell equipped with an inlet and outlet ports for gas transport and solution sampling, respectively. The top of the cell was sealed with a quartz window (JGS2). Solutions were irradiated from above by simulated sunlight using a Xenon lamp coupled with an optical fiber (CEL-TCX250, Beijing China Education Au-light Co., Ltd.), and a water filter was used in front of the radiation source. The reason is that both solar irradiation and xenon lamp irradiation contain a small fraction (<5%) of UV light (Niu et al., 2013). To further explore the reaction mechanisms, irradiation was also conducted by a high-pressure mercury lamp (MERC500, NBet Technology Co., Ltd) coupled with a 313 nm UV optical filter. And 8 mW/cm^2 (measured by an UV light meter, LS125-UVB, Linshang Technology Co., Ltd) was selected as the experimental light intensity after the pre-experiment, which could also achieve the expected results. A thermostatic water bath circulating water through the reactor jacket was used to keep the temperature constant at 25 °C.

Measurements of SO_4^{2-} and NO_x. During the reaction, liquid samples were taken out at given time intervals (0, 20, 40, …, 120 min) and 0.1 mL 2-propanol was added to each sample to suppress the continuous oxidation by oxygen in the air during the test process (Braga and Connick, 1982; Alyea and Bäckström, 1929). Then these samples were analyzed by an ion chromatography (940 Professional IC Vario, Metrohm, Switzerland), which was equipped with a separation column of Metrosep A supp 5-250

https://doi.org/10.5194/acp-2020-806
Preprint. Discussion started: 31 August 2020

and a Metrosep A supp 5 S guard column for anion, and a Metrosep C 6-150 analytical column and a Metrosep C 6 guard column for cation. 5% acetone was added to the anion eluent to distinguish the peaks of sulfite and sulfate, so as to obtain the accurate content of sulfate in the sample. Detection of NO_x was conducted in the absence of bisulfite. Nitrogen bubbling was used to help the produced NO_x escaped from the solution, and then NO_x was measured using a NO-NO_2-NO_x analyzer (42i, Thermo Scientific, USA).

■ RESULTS AND DISCUSSION

Aqueous Oxidation of Bisulfite by Nitrate Photolysis. NH_4NO_3 and $(NH_4)_2SO_4$ are the major constituents of atmospheric particulate matter (Sun et al., 2013). Thus, NH_4NO_3 was selected as the source of nitrate in this study (Shen et al., 2012). The aqueous oxidation of bisulfite influenced by nitrate photolysis was carried out under different conditions, as shown in Figure 1(a). The reaction with nitrate and light (S1, 13.58 $\mu M \cdot min^{-1}$) has a higher sulfate formation within 120 min than that in the dark (S2, 13.00 $\mu M \cdot min^{-1}$), verifying the promotion of nitrate photolysis on HSO_3^- oxidation. Considering the insignificant increase of sulfate yield, experiments were conducted under 313 nm UV light (Figure 1(b)) again to explore the reaction mechanisms. Sulfate formation remarkably enhanced in the presence of nitrate photolysis (S'1, 63.80 $\mu M \cdot min^{-1}$) compared with the low yield in dark. It may be attributed to the oxidation of HSO_3^- by various oxidizing species produced by nitrate photolysis, such as •OH (Gen et al., 2019b; Mack and Bolton, 1999). •OH can be produced directly (R3) (Scharko et

https://doi.org/10.5194/acp-2020-806
Preprint. Discussion started: 31 August 2020

al., 2014), or via indirect pathway induced by nitrate photolysis (R4-10) (Li et al., 2018b; Yabushita et al., 2008; Ye et al., 2016; Bao et al., 2018): A simulated solar irradiation of an aqueous solution of nitrate generates O^- that readily reacts with H^+ to form •OH. The secondary photolysis of HONO produced from nitrate photolysis (R6-R8) is also a source of •OH, and the photo-formation of •OH from HONO and NO_2^- is pH dependent (Arakaki et al., 1999). It should be pointed out that the indirect pathways for •OH formation processes include photoisomerization of nitrate to produce intermediate peroxynitrite ($ONOO^-$) as well, which can combine with H^+ to form peroxynitrous acid (HOONO). HOONO can produce •OH upon decomposition but $ONOO^-$ does not, and hence a decrease of pH would enhance the yield of •OH photoproduction (Mack and Bolton, 1999), which favors the oxidation of HSO_3^-. The contribution of •OH to sulfate formation was discussed later. NO_2, another direct product of nitrate photolysis (R3 and R4), is also a key factor that leads to HSO_3^- oxidation. HSO_3^- is oxidized by NO_2 directly (R11) or indirectly (R12) (Li et al., 2018b; Cheng et al., 2016; Guo et al., 2017; Clifton et al., 1988; Gen et al., 2019a). The NO_x analysis results in Figure 2 show that NO_2 is generated rapidly and the yield reached the maximum (~ 54 ppb) within 20 min, and then maintained at a relatively stable rate. The simultaneous formation of NO is due to the photolysis of partial NO_2 and HONO (R13 and R14). Additionally, the intermediate products such as nitrite (NO_2^-) and nitrous acid (HONO), i.e., N(III) species are also considered as the contributors of aqueous phase SO_2 oxidation for sulfate formation as well by previous studies (Gen et al., 2019a; Li et al., 2018b; Kong et al., 2014). And even N(III) species was considered as the main contributors to the

https://doi.org/10.5194/acp-2020-806
Preprint. Discussion started: 31 August 2020

heterogeneous SO_2 aqueous phase oxidation under 300 nm irradiation, followed by NO_2 contribution (Gen et al., 2019a). Therefore, the enhanced sulfate formation in this study is a combined result of the oxidation of bisulfite by various oxidizing species produced by the photolysis of nitrate.

The direct oxidation of HSO_3^- by O_2 cannot be ignored according to S3 (8.74 $\mu M \cdot min^{-1}$). Meanwhile, compared to S'1, the low sulfate formation influenced by nitrate photolysis under oxygen-free condition (S'4, 11.92 $\mu M \cdot min^{-1}$) indicates the key role of oxygen for the process of nitrate photolysis affecting the conversion of HSO_3^-. Details were discussed later. And no obvious sulfate generation in the absence of ammonium nitrate and O_2 (S5) was observed. The small amount of sulfate increment is attributed to the oxidation of HSO_3^- by some dissolved O_2 in the solution. Another interesting result was found via the comparison between S2 (13.00 $\mu M \cdot min^{-1}$) and S3 (8.74 $\mu M \cdot min^{-1}$), that is, nitrate itself can greatly promote the oxidation of bisulfite in the solution under dark condition. This result is consistent with our previous study in which nitrate facilitates the heterogeneous conversion of SO_2 on humid hematite particles in the dark (Kong et al., 2014). Furthermore, this result also confirms our previous finding that high-nitrate haze episodes favor the heterogeneous aqueous oxidation of SO_2 and the formation of sulfate (Kong et al., 2018). Additionally, state-of-the-art air quality models that rely on sulfate production mechanisms requiring photochemical oxidants fail to predict the high levels of sulfate because the sunlight is usually thought to be weak during haze events (Cheng et al., 2016), this may provide a reasonable explanation for the enhanced conversion of atmospheric SO_2 and the

https://doi.org/10.5194/acp-2020-806
Preprint. Discussion started: 31 August 2020

enhanced formation of secondary sulfate aerosols observed in severe haze episodes with very weak radiation.

Effect of pH on Sulfate Formation. pH is an important factor affecting the aqueous phase formation of sulfate (Barth et al., 2000), and then its effect on the reaction was investigated. The pH of initial solution was 4.32 when the concentrations of $NaHSO_3$ and NH_4NO_3 were both 30 mM. Hence, the formation of sulfate discussed before confirms the occurrence of nitrate photolysis under acidic conditions, as reported by earlier works (Gen et al., 2019b; Scharko et al., 2014; Benedict et al., 2017). Additionally, ammonium sulfate (AS), a salt of a strong acid and a weak base, is the main form of atmospheric sulfate aerosol (Appel et al., 1978), and ammonium bisulfate (ABS) has a stronger acidity, and thus they will inevitably affect the pH of various aqueous phase system in the atmosphere, such as cloud and fog droplets. Therefore, they were used to further adjust the expected pH value of the reaction solution in different range in this study.

Figure 3(a) shows sulfate formation as a function of pH adjusted by the addition of $(NH_4)_2SO_4$, NH_4HSO_4 and the mixture of $(NH_4)_2SO_4$ and NH_4HSO_4, respectively. As can be seen from Figure 3(a), enhanced sulfate formation is observed in all $(NH_4)_2SO_4$-adjusted systems, and more addition of $(NH_4)_2SO_4$ results in lower pH and more significant sulfate formation. This result not only shows the important role of the pH in sulfate formation, but also indicates a crucial role of ammonium sulfate in regulating pH in the enhancement of sulfate formation. This is of great significance for

https://doi.org/10.5194/acp-2020-806
Preprint. Discussion started: 31 August 2020

understanding the behavior of ammonium sulfate in the atmosphere. On the one hand, the lower pH favors the formation of •OH as described by reactions R3-R10. On the other hand, it may because that NO_3^- under acidic conditions is more easily photolyzed to produce •OH or HONO (Mack and Bolton, 1999; Bao et al., 2018; Turnipseed et al., 1992). As a result, an increasingly enhanced sulfate formation is achieved as the pH decreases. However, totally different results are obtained in NH_4HSO_4-adjusted systems. The oxidation of bisulfite is greatly suppressed when pH < 2.08. One possible explanation is that HSO_3^- concentration is greatly reduced when pH < 2.08 due to the equilibrium of reaction R1, even though nitrate photolysis under acidic conditions continues, which will lead to the reduction of sulfate formation. This result may suggest that there is an optimum pH value for sulfate formation. In addition, the middle range of pH is reached by adding the mixed solution of $(NH_4)_2SO_4$ and NH_4HSO_4, and the enhanced sulfate formation is also observed. Sulfate formation as a function of pH is described in Fig 3(b). As can be seen from it, the pH for the highest sulfate formation is about 3.86, which is within the pH range of atmospheric particles. Generally, atmospheric $PM_{2.5}$ is acidic due to partial neutralization of acidic sulfate and nitrate aerosols under some conditions (Guo et al., 2017; Liu et al., 2017). Liu et al. (2017) found that fine particles were moderately acidic during severe haze episodes in northern China, with a pH range of 3.0-4.9 and an average of 4.2. Guo et al. (2017) observed that the PM_1 pH, regardless of ammonia levels, was always acidic, with an average of 4.2, even for the unusually high NH_3 levels found in Beijing (pH = 4.5). Meanwhile, although the sunlight is usually thought to be weak during haze events, field

https://doi.org/10.5194/acp-2020-806
Preprint. Discussion started: 31 August 2020

observations showed that the photochemical reactivity during the winter or haze episodes is still relatively high (Ye et al., 2018; Tan et al., 2018). Therefore, this result suggests the new aqueous phase oxidation pathways coupled with nitrate photolysis, which may play significant roles in the formation of secondary sulfate and the occurrence and evolution of haze episodes in China.

Additionally, under the same conditions, the comparison of $NaNO_3$ as the source of NO_3^- for sulfate formation was carried out. Different conclusion from Gen et al. was drew, who believed that the type of cation has little influence on nitrate photolysis (Gen et al., 2019a). As can be seen from Fig 4, sulfate yields with $NaNO_3$ photolysis are both lower than that with NH_4NO_3 at the same concentration, for that the hydrolysis of NH_4^+ may maintain a stable and low pH of the solution during the process, which is more conducive to the formation of sulfate as described by R3-R10. Meanwhile, the same low sulfate yields by photolysis of $NaNO_3$ and NH_4NO_3 at pH < 2 verify that too low pH is unfavorable to sulfate formation again. To further investigate the role of NH_4^+, the photolysis of NO_3^- with different NH_4^+ content was conducted within the optimum pH range. Results in Fig S1 show that sulfate yield increases with the increase of NH_4^+ content, revealing the significant role of NH_4^+ on the reaction. This may be because that $NH_3{\bullet}H_2O_{(aq)}$ and/or $NH_{3(aq)}$, which were produced by the hydrolysis of NH_4^+ (RS1), can be oxidized by nitrate photolysis product NO_2 (RS2-RS5), and thus the shift of chemical equilibrium enhances the photolysis of nitrate and the generation of •OH. Also, the standard Gibbs energy of formation for the two reactions indicate that the oxidation reactions of $NH_3{\bullet}H_2O_{(aq)}$ and $NH_{3(aq)}$ by NO_2 are spontaneous ($\Delta_f G^\circ < 0$, listed in Text

https://doi.org/10.5194/acp-2020-806
Preprint. Discussion started: 31 August 2020

S2). Therefore, the generation of •OH enhances simultaneously, thus leading to the increased sulfate formation. In addition, it is reported that NH_3 can promote the hydrolysis of NO_2 and induce the explosive growth of HONO via reaction R6 by reducing the free energy barrier of the reaction and stabilizing the product state (Li et al., 2018a; Xu et al., 2019). The HONO produced releases •OH upon photolysis (R10). The highly oxidative free radicals promote the formation of sulfate. These results reflect the crucial role and contribution of ambient widely-existing ammonium sulfate in the formation of sulfate aerosols and photochemical pollution in the atmosphere.

Role of O_2 and •OH in the aqueous oxidation of bisulfite. As mentioned, O_2 and •OH play important roles in the oxidation of HSO_3^-. We discussed it further here. It is reported that alcohols can be used as inhibitors of sulfite and bisulfite oxidation (Braga and Connick, 1982; Alyea and Bäckström, 1929). Braga and Connick found that the oxidation of S(IV) by O_2 is a chain reaction, and alcohols can inhibit the reaction by chain termination (Braga and Connick, 1982), but Alyea and Bäckström claimed that the oxidation of the S(IV) induces the oxidation of alcohols and the alcohols can be easily oxidized to aldehydes and ketones (Alyea and Bäckström, 1929). In addition, in the presence of 2-propanol, •OH reacts primarily with 2-propanol ($k=1.9\times10^9$ $M^{-1}s^{-1}$) through α-hydrogen abstraction generating 1-hydroxy-1-methylethyl radical, while at lower concentrations of 2-propanol, the scavenging reaction of •OH with H_2O_2 (R15) become competitive (Hislop and Bolton, 1999). The formation of H_2O_2 in the reaction systems will be discussed later. Therefore, in this study, 2-propanol was added to

https://doi.org/10.5194/acp-2020-806
Preprint. Discussion started: 31 August 2020

investigate the role of O_2 and •OH in the aqueous oxidation of bisulfite. The results are presented in Fig 5. As can be seen from Fig.5, a slight reduction of sulfate formation after the addition of 2-propanol was observed in the dark, indicating the suppression of 2-propanol on the oxidation of HSO_3^- by O_2 because that 2-propanol can inhibit the chain reaction between HSO_3^- and O_2 by chain termination (Braga and Connick, 1982), or be easily oxidized by O_2 induced by the oxidation of HSO_3^- (Alyea and Bäckström, 1929), as mentioned before. The inconspicuous inhibition showed that O_2 oxidation is not the main direct contributor on the aqueous phase oxidation of bisulfite in the presence of nitrate.

However, as proved before, O_2 is of great significance on nitrate photolysis for the conversion of HSO_3^-. On the one hand, the inhibition of 2-propanol on sulfate yield in the presence and absence of O_2 under light were similar (Figure 5), demonstrating that O_2 has little effect on the generation of •OH by nitrate photolysis. This is definitely distinct with previous report by Gen et al. (2019b), who found that •OH is generated in the presence of O_2. Furthermore, they claimed that the contribution of •OH pathway on the oxidation of dissolved SO_2 was almost absent (<1%) under nitrate photolysis at 300 nm (Gen et al., 2019a). In our study, 8.59% and 25.02% of sulfate formation in the presence and absence of O_2 respectively under 313 nm irradiation were owing to the •OH oxidation, which is not obviously negligible. The quantum yield of •OH ($\Phi_{\bullet OH}$) was measured further (Text S4). The calculated $\Phi_{\bullet OH}$ in Table 1 shows that lower pH facilitates the generation of •OH during nitrate photolysis, verifying the points discussed before again. However, considering that the •OH would be recombined to

https://doi.org/10.5194/acp-2020-806
Preprint. Discussion started: 31 August 2020

form H_2O_2 (discussed in next section) during its generation process, the calculated $\Phi_{\bullet OH}$ is not the completely accurate one.

In addition, it is reasonably inferred that O_3 was generated during nitrate photolysis and became an important contributor for sulfate formation. As is known to all that in aqueous solution $O(^3P)$ (one of the products of nitrate photolysis, R5) can react with molecular oxygen to form ozone similar to the gas phase (R16) (Herrmann, 2007). Therefore, it is expected that HSO_3^- will be oxidized by O_3, but this still needs further study.

Generation of hydrogen peroxide during the photolysis process

Previous studies haven't detected H_2O_2 during steady-state irradiation of NO_2^- and NO_3^- solutions at $\lambda > 200$ nm (Daniels et al., 1968; Shuali et al., 1969; Mark et al., 1996), but Wagner et al. once found H_2O_2 formation in flash photolysis of nitrate ions in acidic aqueous solution (Wagner et al., 1980). However, Mack et al. thought that the combination reaction between two •OH produced by nitrate photolysis is highly unlikely due to the very low concentration and short lifetime of •OH, and they attributed the formation of H_2O_2 observed by Wagner et al. to the H_2O photolysis at $\lambda > 180$ nm (Mack and Bolton, 1999). However, Yabushita et al. (2008) once again found that the produced •OH by the photolysis of nitrate originated from the adsorption of nitric acid can recombine to form H_2O_2 under low-temperature ice conditions.

H_2O_2 generation during the photochemical process of nitrate was verified in this study. H_2O_2 was measured by titanium (III) sulfate spectrophotometry and the results

https://doi.org/10.5194/acp-2020-806
Preprint. Discussion started: 31 August 2020

are depicted in Fig S2. The production of H_2O_2 shows a trend of increasing first and then decreasing, which is due to the fact that H_2O_2 is photodegraded as its formation. Considering the contributions of NH_4^+ and pH, and the absence of precursor of hydroperoxyl radical (HO_2) in our reaction system, we can speculate that the formation of H_2O_2 is owing to the recombination of •OH originated from nitrate photolysis and it may make an important contribution to HSO_3^- oxidation and sulfate formation. When 25 mM $(NH_4)_2SO_4$ and NH_4HSO_4 added, the pH of solution decreased from 5.00 to 4.63 and 0.97 respectively, as a result, H_2O_2 formation is found to be remarkably pH-dependent. The formation of H_2O_2 displayed a higher efficiency at a lower pH, which indicates that lower pH favors the photolysis of nitrate to generate •OH and the formation of H_2O_2. These may reveal the new formation pathways to the source of H_2O_2 in cloud, fogs and liquid haze particles, which may be important for the conversion of atmospheric SO_2 and the formation of atmospheric sulfate, as well as the occurrence and evolution of haze events. Such aspects need to be further explored in future.

Effect of light intensity on aqueous phase formation of sulfate.

Although sunlight is dimmed by ambient PM during haze events, it is not completely absent (Xia et al., 2018), and the active photochemistry is also found during the winter or haze episodes and facilitates the production of secondary pollutants (Lu et al., 2019). In the late period of haze events with weak solar radiation, significant increase of sulfate and nitrate was observed (Quan et al., 2015). In order to reveal the impact of the solar radiation on sulfate formation through the aqueous phase pathways we mentioned

https://doi.org/10.5194/acp-2020-806
Preprint. Discussion started: 31 August 2020

above, we carried out experiments under a higher light intensity. As shown in Fig S5, a higher light intensity more favors sulfate formation than that under 8 mW/cm^2 irradiation.

Role of Halide Ions in Aqueous Phase Oxidation of Bisulfite. Field observations indicate that nitrate ions commonly coexist with halide ions in aged sea salt particles and atmospheric particles due to the transport of sea salt aerosols, the emission of fossil fuel combustion and biomass burning. Our previous study verified that high-nitrate haze episodes occurred in Shanghai (a coastal mega-city) favored heterogeneous aqueous oxidation of SO_2 (Kong et al., 2018). However, little is known about the role of halide ions in the heterogeneous aqueous oxidation of SO_2 and the formation of sulfate. Therefore, the role of halide ions in the aqueous phase oxidation of HSO_3^- under nitrate photolysis was further investigated. Results in Fig 7(a) show that sulfate formation is evidently enhanced in the presence of halide ions X^- or Y^- (X, Y: Cl, Br and I), indicating the promotion effect of halide ions on aqueous phase oxidation of bisulfite in the presence of nitrate and light.

In this study, halide-induced enhancement of nitrate photolysis for sulfate formation owing to halide photochemistry and the redox cycle of halogen was proposed for the first time. Firstly, direct photolysis of X^- generates $X^\bullet$, followed by the rapid reaction of $X^\bullet$ with halide ion X^- (or Y^-) to form $X_2^{\bullet -}$ (or $XY^{\bullet -}$) as reaction R17 and R18 (Zhang and Parker, 2018). Secondly, halide ions can be oxidized by nonhalogen radicals from nitrate photolysis and the free radical chain oxidation of S(IV) [e.g. •OH (R19); sulfate

https://doi.org/10.5194/acp-2020-806
Preprint. Discussion started: 31 August 2020

radical, $SO_4^{\bullet -}$ (R21)] to generate halogen radicals, and halogen radicals are present at higher concentrations relative to •OH in more acidic solutions (Zhang and Parker, 2018), as indicated by reaction R19-R22. Additionally, peroxymonosulfuric acid (HSO_5^-) produced by the free radical chain oxidation of S(IV) is known to react with halide ions to produce HOX (Mozurkewich, 1995), e.g. reaction R23, and then HOX photolysis generates $X^\bullet$ and •OH (reaction R24). Nonradical halogen oxidant products X_2 and HOX can also be formed from rapid reactions R25-R29 (Zhang and Parker, 2018). And, the reaction of HOBr with Br^- (or Cl^-) can also lead to the production of Br_2 (or BrCl), as described by R30 and R31 (Mozurkewich, 1995; Vogt et al., 1996). Moreover, •OH can oxidize both Cl^- and Br^- to form photochemically active halogen molecules such as Br_2, BrCl and Cl_2 (R32-R34) (Alexander et al., 2003; Richards and Finlayson-Pitts, 2012; Richards-Henderson et al., 2013). In addition, Br^- can be oxidized to Br_2 by nitrate under acidic conditions in the dark (R35), and the formed HONO further oxidizes Br^- (Richards-Henderson et al., 2013). These nonradical halogen oxidant products may contribute to subsequent oxidation of HSO_3^- (R36, R37), e.g., rapid S(IV) oxidation by HOCl and HOBr (R38, R39) (Richards and Finlayson-Pitts, 2012; Vogt et al., 1996). It should be noted that althrough the direct photolysis of halide ions exists, this pathway may play a small role in our study because the used xenon lamp emits very few specific wavelengths for the reaction.

Therefore, in this study, compared to that in the absence of halide ions, extra oxidations caused by the introduction of halide ions significantly promote the conversion of HSO_3^- and the formation of sulfate, showing an apparent synergism

https://doi.org/10.5194/acp-2020-806
Preprint. Discussion started: 31 August 2020

among halogen chemistry, nitrate photolysis and S(IV) aqueous oxidation. Herein, it should point out that the redox cycle of halogen for the oxidation of HSO_3^- under nitrate photolysis exists. That is, the oxidants HOX and X_2 produced by the oxidation of halide ions react with bisulfite to generate sulfate as well as to regenerate halide ions, thus forming a redox cycle of halogen to achieve the continuous oxidation conversion of bisulfite. Halide ions act as catalysts in the cyclic reactions. Furthermore, Fig 7(a) also shows that the sulfate yields of the three groups with the addition of Cl^-, Br^- and I^- exhibit an increasing tendency, especially the one with added I^-, which is much higher than that of the Cl^- and Br^-. On the one hand, pH plays a key role. The pH of bulk solution with addition of Cl^-, Br^- and I^- are 4.42, 4.20 and 3.60, respectively. As depicted in Fig 3(b) the lower pH of the three favors sulfate formation. On the other hand, sulfate yields present an order of Cl^--added system<Br^--added system<I^--added system, which is consistent with their reducibility. Compared with Cl_2/Cl^- and Br_2/Br^- redox cycles, the formed I_2 has stronger oxidizability, and I^- has stronger reducibility, and thus it is easier to form I_2/I^- (or I_3^-/I^-) redox cycle in our reaction system, resulting in a higher sulfate yield. In addition, it is noteworthy that the added halide ions promote the aqueous phase oxidation of HSO_3^- in the dark as well, as can be seen from Fig 7(b). But the sulfate yield of dark reaction with different X^- is lower than that with light. This result indicates the simultaneous contributions of the decreased pH and the redox cycle of halogen originated from the reaction R22, R23 and R35 and the aqueous phase oxidation of HSO_3^- in the absence of light. Similarly, the autocatalytic reaction of this system is achieved as well in the dark.

https://doi.org/10.5194/acp-2020-806
Preprint. Discussion started: 31 August 2020

The results suggest that the redox cycle of halogen caused by the nitrate and its photochemistry as well as HSO_5^- will be coupled with the aqueous phase oxidation process of SO_2 to greatly promote the formation of sulfate, both under the light and dark conditions, which is of great significance to understand the impacts of sea salt aerosol in coastal areas of China and the halide ions from coal combustion in northern areas of China on the formation of secondary aerosols and the occurrence and evolution of haze episodes or air pollution in China. Additionally, the transport of biomass burning can induce air pollution and haze episodes in the receptor areas by the significantly enhanced formation of secondary sulfate and nitrate aerosols (Du et al., 2011; Tong et al., 2020). The interactions between the plume of biomass burning and local pollutants are often used to explain the enhanced secondary aerosol formation, but the real reason remain unclear. Therefore, the role of halogen chemistry we studied may provide a reasonable explanation for the occurrence of haze episodes induced by biomass burning. These lay a foundation for us to extend the relevant research to the formation of atmospheric SOA and organic halides in the future.

CONLUSIONS AND ATMOSPHERIC IMPLICATIONS

The effects of nitrate photolysis on the aqueous phase oxidation of bisulfite under different conditions have been investigated. A combining contribution of various oxidizing species (•OH, NO_2, NO_2^- and HONO, etc.) produced via the photolysis of nitrate achieves the enhanced oxidation of bisulfite and the enhanced sulfate formation. pH plays a significant role in bisulfite oxidation and sulfate formation. The highest

https://doi.org/10.5194/acp-2020-806
Preprint. Discussion started: 31 August 2020

sulfate formation occurs in the range of moderate acidity, about 3.86, which is within the pH range of atmospheric particles. Furthermore, NH_4^+ promotes the generation of •OH and thus enhances the formation of sulfate, which is attributed to the oxidation of NH_4^+ hydrolysis products NH_3•$H_2O_{(aq)}$ and $NH_{3(aq)}$ by NO_2, and the promotion role of NH_4^+ hydrolysis products in the hydrolysis of NO_2 to form HONO. Additionally, O_2 remarkably facilitates nitrate photolysis for the conversion of HSO_3^-. And H_2O_2 can be generated via the recombination of •OH from nitrate photolysis. More importantly, the redox cycle of halogen coupled with S(IV) oxidation significantly promote the conversion of HSO_3^- and the formation of sulfate under nitrate photolysis or in acidic nitrate solution in the dark, showing the apparent synergism among halogen chemistry, nitrate chemistry and S(IV) aqueous oxidation. Our study verifies that S(IV) oxidation can be coupled not only with nitrate and its photochemistry, but also with the redox cycle of halogen, which greatly promotes the formation of sulfate.

Results from this study have important atmospheric implications. Firstly, in recent years in China, photochemical pollution and haze episodes have occurred more frequently and the haze episodes with high nitrate level are increasingly apparent. Due to the relatively high RH and high concentrations of particulate nitrate, the aerosol is mostly in the aqueous phase during haze episodes (Liu et al., 2017b; Kong et al., 2018; Lu et al., 2019). Meanwhile, sunlight is not completely absent during haze episodes (Ye et al., 2018; Xia et al., 2018), and the active photochemistry is also found during the winter or haze episodes and facilitates the production of secondary pollutants (Lu et al., 2019). Therefore, the enhanced aqueous phase oxidation of bisulfite and the enhanced

https://doi.org/10.5194/acp-2020-806
Preprint. Discussion started: 31 August 2020

formation of sulfate under the coupling with nitrate photolysis or in the nitrate solution under dark condition may occur in the haze episodes and promote the occurrence and evolution of haze episodes in China. In the meantime, the important roles of ammonium sulfate in regulating the pH of solution and the enhancement of sulfate production will also be reflected.

Secondly, nitrate aerosol is ubiquitous in the atmosphere, and it will inevitably mix with halide ions (X^- = Cl^-, Br^-, I^-) from sea salt particles, coal combustion and biomass burning, especially over the coastal areas and the northern areas of China. The typical haze areas in China include Beijing-Tianjin-Hebei area, Yangtze River Delta area and Pearl River Delta area, the three coastal areas in nature, which may suggest the potential roles of halide ions in the occurrence and evolution of hazes. Therefore, the reactions such as those reported here may occur in aqueous phase aerosols (e.g. fog and cloud droplets) or aerosol particles with water film, and the formation of $X\cdot$, NO_2, HOX, X_2, XY or the X_2/X^- redox cycle will further enhance the conversion of SO_2 and/or oxidation of organic gaseous precursors, thus promoting the occurrence and evolution of air pollution or haze. Our study highlights the roles of halide ions in the formation of secondary aerosols and air pollution. Meanwhile, the formed $X\cdot$, X_2 or XY may be liberated from the aqueous phase particles or the particles with water film into the air, and thus they will affect the tropospheric O_3 level.

Finally, secondary organic aerosol (SOA) is also an important component of atmospheric aerosols, and it has attracted much attention all the time. Our investigation provides a case study on the formation of secondary inorganic aerosols, which can be

https://doi.org/10.5194/acp-2020-806
Preprint. Discussion started: 31 August 2020

extended to the study on the influences of nitrate photochemistry and the coupled redox cycle of halogen on the formation of SOA, such as the hydroxylation and halogenation of organic substrates, etc.

■ ASSOCIATED CONTENT

Supporting Information

■ AUTHOR INFORMATION

Corresponding Author

*E-mail: ldkong@fudan.edu.cn

ORCID

Notes

The authors declare no competing financial interest.

■ AUTHOR CONTRIBUTION

Lingdong Kong, as a tutor, guided and provided suggestions in the whole research process. Lu Chen undertook the main experiment and prepared the manuscript with contributions from all co-authors. Songying Tong and Kejing Yang provided guidance on experimental instruments and their operation methods. Shengyan Jin and Chao Wang carried out some basic experiments. And Lin Wang provided a part of financial support on instruments and materials.

■ ACKNOWLEDGEMENTS

This study was supported by the National Natural Science Foundation of China (Grant Nos. 21777027 and 21976032) and the National Key R & D Program of China (2017YFC0209505).

https://doi.org/10.5194/acp-2020-806
Preprint. Discussion started: 31 August 2020

■ REFERENCES

Alexander, L., Gaspar, D. J., Weihong, W., Hunt, S. W., Cowin, J. P., Colson, S. D., and Finlayson-Pitts, B. J.: Reactions at interfaces as a source of sulfate formation in sea-salt particles, Science, 301, 340-344, https://doi.org/10.1126/science.1085374, 2003.

Alyea, H. N., and Bäckström, H. L. J.: The inhibitive action of alcohols on the oxidation of sodium sulfite, J. Am. Chem. Soc, 51, 90-109, https://doi.org/10.1021/ja01376a011, 1929.

Appel, B. R., Kothny, E. L., Hoffer, E. M., Hidy, G. M., and Wesolowski, J. J.: Sulfate and nitrate data from the California Aerosol Characterization Experiment (ACHEX), Environ. Sci. Technol, 12, 418-425, https://doi.org/10.1021/es60140a005, 1978.

Arakaki, T., Miyake, T., Hirakawa, T., and Sakugawa, H.: pH dependent photoformation of hydroxyl radical and absorbance of aqueous-phase N(III) (HNO_2 and NO_2^-), Environ. Sci. Technol, 33, 2561-2565, https://doi.org/10.1021/es980762i, 1999.

Bao, F., Li, M., Zhang, Y., Chen, C., and Zhao, J.: Photochemical aging of Beijing urban PM2.5: HONO production, Environ. Sci. Technol, 52, 6309-6316, https://doi.org/10.1021/acs.est.8b00538, 2018.

Barth, M. C., Rasch, P. J., Kiehl, J. T., Benkovitz, C. M., and Schwartz, S. E.: Sulfur chemistry in the National Center for Atmospheric Research Community Climate Model: Description, evaluation, features, and sensitivity to aqueous chemistry, J. Geophys. Res. Atmos, 105, 1387-1415, http://dx.doi.org/10.1029/1999JD900773, 2000.

Benedict, K. B., McFall, A. S., and Anastasio, C.: Quantum yield of nitrite from the photolysis of aqueous nitrate above 300 nm, Environ. Sci. Technol, 51, 4387-4395, https://doi.org/10.1021/acs.est.6b06370, 2017.

Braga, T. G., and Connick, R. E.: Kinetics of the oxidation of bisulfite ion by oxygen, in: Flue Gas Desulfurization, ACS Symposium Series, 188, American Chemical Society, 153-171, http://dx.doi.org/10.1021/bk-1982-0188.ch008, 1982.

Cahill, T. A., Wilkinson, K., and Schnell, R.: Composition analyses of size-resolved aerosol samples taken from aircraft downwind of Kuwait, spring 1991, J. Geophys. Res. Atmos, 97, 14513-14520, http://dx.doi.org/10.1029/92JD01373, 1992.

Cheng, Y., Zheng, G., Wei, C., Mu, Q., Zheng, B., Wang, Z., Gao, M., Zhang, Q., He, K., Carmichael, G., Pöschl, U., and Su, H.: Reactive nitrogen chemistry in aerosol water as a source of sulfate during haze events in China, Sci Adv, 2, http://dx.doi.org/e1601530-e1601530, 10.1126/sciadv.1601530, 2016.

Cheng, Z. L., Chan, L. W. T., Cheng, K. K., and Lam, K. S.: Chemical characteristics of aerosols at coastal station in Hong Kong. I. Seasonal variation of major ions, halogens and mineral dusts between 1995 and 1996, Atmos. Environ, 34, 2771-2783, http://dx.doi.org/10.1016/S1352-2310(99)00343-X, 2000.

Clifton, C. L., Altstein, N., and Huie, R. E.: Rate constant for the reaction of nitrogen dioxide with sulfur(IV) over the pH range 5.3-13, Environ. Sci. Technol, 22, 586-589, http://dx.doi.org/10.1021/es00170a018, 1988.

Custard, K. D., Raso, A. R. W., Shepson, P. B., Staebler, R. M., and Pratt, K. A.: Production and release of molecular bromine and chlorine from the arctic coastal snowpack, ACS. Earth. Space. Chem, 1, 142-151, http://dx.doi.org/10.1021/acsearthspacechem.7b00014, 2017.

Daniels, M., Meyers, R. V., and Belardo, E. V.: Photochemistry of the aqueous nitrate system. I. Excitation in the 300-m.mu. band, J. Phys. Chem, 72, https://doi.org/10.1021/j100848a002, 1968.

Du, C., Kong, L., Zhanzakova, A., Tong, S., Yang, X., Wang, L., Fu, H., Cheng, T., Chen, J., and Zhang, S.: Impact of adsorbed nitrate on the heterogeneous conversion of SO_2 on alpha-Fe_2O_3 in the absence and presence of simulated solar irradiation, Sci. Total. Environ, 649, 1393-1402, http://dx.doi.org/10.1016/j.scitotenv.2018.08.295, 2019.

Du, H., Kong, L., Cheng, T., Chen, J., Du, J., Li, L., Xia, X., Leng, C., and Huang, G.: Insights into summertime haze pollution events over Shanghai based on online water-soluble ionic composition of aerosols, Atmos. Environ, 45, 5131-5137, http://dx.doi.org/10.1016/j.atmosenv.2011.06.027, 2011.

Dubowski, Y., Colussi, A. J., and Hoffmann, M. R.: Nitrogen dioxide release in the 302 nm band photolysis of spray-frozen aqueous nitrate solutions. Atmospheric implications, J. Phys. Chem. A, 105, 4928-4932, http://dx.doi.org/10.1021/jp0042009, 2001.

Gen, M., Zhang, R., Huang, D. D., Li, Y., and Chan, C. K.: Heterogeneous oxidation of SO_2 in sulfate production during nitrate photolysis at 300 nm: Effect of pH, relative humidity, irradiation intensity, and the presence of organic compounds, Environ. Sci. Technol, 53, 8757-8766, http://dx.doi.org/10.1021/acs.est.9b01623, 2019a.

Gen, M., Zhang, R., Huang, D. D., Li, Y., and Chan, C. K.: Heterogeneous SO_2 oxidation in sulfate formation by photolysis of particulate nitrate, Environ. Sci. Technol. Lett, 6, 86-91, http://dx.doi.org/10.1021/acs.estlett.8b00681, 2019b.

Gligorovski, S., Strekowski, R., Barbati, S., and Vione, D. J. C. R.: Environmental implications of hydroxyl radicals (•OH), Chem. Rev, 115, 13051-13092, http://dx.doi.org/10.1021/cr500310b, 2015.

Guo, H., Weber, R. J., and Nenes, A.: High levels of ammonia do not raise fine particle pH sufficiently to yield nitrogen oxide-dominated sulfate production, Sci. Rep, 7, 12109, http://dx.doi.org/10.1038/s41598-017-11704-0, 2017.

Guo, S., Hu, M., Levy Zamora, M., Peng, J., Shang, D., Zheng, J., Du, Z., Wu, Z., Shao, M., Zeng, L., Molina, M., and Zhang, R.: Elucidating severe urban haze formation in China, P. Natl. Acad. Sci. USA, http://dx.doi.org/111, 10.1073/pnas.1419604111, 2014.

Herrmann, H.: On the photolysis of simple anions and neutral molecules as sources of O^-/OH, SO_x^- and Cl in aqueous solution, Phys. Chem. Chem. Phys, 9, 3935-3964, http://dx.doi.org/10.1039/b618565g, 2007.

Hislop, K. A., and Bolton, J. R.: The photochemical generation of hydroxyl radicals in the UV-vis/Ferrioxalate/H_2O_2 system, Environ. Sci. Technol, 33, 3119-3126, http://dx.doi.org/10.1021/es9810134, 1999.

Hoffman, R. C., Laskin, A., and Finlayson-Pitts, B. J.: Sodium nitrate particles: physical and chemical properties during hydration and dehydration, and implications for aged sea salt aerosols, J. Aerosol. Sci, 35, 869-887, http://dx.doi.org/10.1016/j.jaerosci.2004.02.003, 2004.

Hua, W., Chen, Z., Jie, C., Kondo, Y., Hofzumahaus, A., Takegawa, N., Lu, K., Miyazaki, Y., Kita, K., and Wang, H.: Atmospheric hydrogen peroxide and organic hydroperoxides during PRIDE-PRD'06, China: their concentration, formation mechanism and contribution to secondary aerosols, Atmos. Chem. Phys, 8, 6755-6773, https://doi.org/10.5194/acp-8-6755-2008, 2008.

Huang, R. J., Zhang, Y., Bozzetti, C., Ho, K. F., Cao, J. J., Han, Y., Daellenbach, K. R., Slowik, J. G., Platt, S. M., Canonaco, F., Zotter, P., Wolf, R., Pieber, S. M., Bruns, E. A., Crippa, M., Ciarelli, G., Piazzalunga, A., Schwikowski, M., Abbaszade, G., Schnelle-Kreis, J., Zimmermann, R., An, Z., Szidat, S., Baltensperger, U., Haddad, I. E., and Prévôt, A. S. H.: High secondary aerosol contribution to particulate pollution during haze events in China, Nature, 514, 218,

https://doi.org/10.1038/nature13774, 2014.

Ibusuki, T., and Takeuchi, K.: Sulfur dioxide oxidation by oxygen catalyzed by mixtures of manganese (II) and iron (III) in aqueous solutions at environmental reaction conditions, Atmos. Environ, 21, 1555-1560, http://dx.doi.org/10.1016/0004-6981(87)90317-9, 1987.

Ji, D., Li, L., Wang, Y., Zhang, J., Cheng, M., Sun, Y., Liu, Z., Wang, L., Tang, G., Hu, B., Chao, N., Wen, T., and Miao, H.: The heaviest particulate air-pollution episodes occurred in northern China in January, 2013: Insights gained from observation, Atmos. Environ, 92, 546-556, http://dx.doi.org/10.1016/j.atmosenv.2014.04.048, 2014.

Kong, L., Du, C., Zhanzakova, A., Cheng, T., Yang, X., Wang, L., Fu, H., Chen, J., and Zhang, S.: Trends in heterogeneous aqueous reaction in continuous haze episodes in suburban Shanghai: An in-depth case study, Sci. Total. Environ, 634, 1192-1204, http://dx.doi.org/10.1016/j.scitotenv.2018.04.086, 2018.

Kong, L. D., Zhao, X., Sun, Z. Y., Yang, Y. W., Fu, H. B., Zhang, S. C., Cheng, T. T., Yang, X., Wang, L., and M., C. J.: The effects of nitrate on the heterogeneous uptake of sulfur dioxide on hematite, Atmos. Chem. Phys., 14, 9451–9467, http://dx.doi.org/10.5194/acp-14-9451-2014, 2014.

Li, L., Huang, C., Huang, H., Wang, Y., Yan, R., Zhang, G., Zhou, M., Lou, S., Tao, S., and Wang, H. J. A. e.: An integrated process rate analysis of a regional fine particulate matter episode over Yangtze River Delta in 2010, Atmos. Environ, 91, 60-70, http://dx.doi.org/10.1016/j.atmosenv.2014.03.053, 2014.

Li, L., Duan, Z., Li, H., Zhu, C., Henkelman, G., Francisco, J. S., and Zeng, X. C.: Formation of HONO from the NH_3-promoted hydrolysis of NO_2 dimers in the atmosphere, Proc. Natl. Acad. Sci. USA, 115, 7236-7241, http://dx.doi.org/10.1073/pnas.1807719115, 2018a.

Li, L., Hoffmann, M. R., and Colussi, A. J.: Role of nitrogen dioxide in the production of sulfate during Chinese haze-aerosol episodes, Environ. Sci. Technol, 52, 2686-2693, http://dx.doi.org/10.1021/acs.est.7b05222, 2018b.

Liu, M., Song, Y., Zhou, T., Xu, Z., Yan, C., Zheng, M., Wu, Z., Hu, M., Wu, Y., and Zhu, T.: Fine particle pH during severe haze episodes in northern China, Geophys. Res. Lett, 44, 5213-5221, http://dx.doi.org/10.1002/2017gl073210, 2017a.

Liu, Y., Wu, Z., Wang, Y., Xiao, Y., Gu, F., Zheng, J., Tan, T., Shang, D., Wu, Y., Zeng, L., Hu, M., P. Bateman, A., and Martin, S.: Submicrometer particles are in the liquid state during heavy haze episodes in the urban atmosphere of Beijing, China, Environ. Sci. Technol. Lett, 4, http://dx.doi.org/10.1021/acs.estlett.7b00352, 2017b.

Lu, K., Fuchs, H., Hofzumahaus, A., Tan, Z., Wang, H., Zhang, L., Schmitt, S. H., Rohrer, F., Bohn, B., Broch, S., Dong, H., Gkatzelis, G. I., Hohaus, T., Holland, F., Li, X., Liu, Y., Liu, Y., Ma, X., Novelli, A., Schlag, P., Shao, M., Wu, Y., Wu, Z., Zeng, L., Hu, M., Kiendler-Scharr, A., Wahner, A., and Zhang, Y.: Fast photochemistry in wintertime haze: Consequences for pollution mitigation strategies, Environ. Sci. Technol, 53, 10676-10684, http://dx.doi.org/10.1021/acs.est.9b02422, 2019.

Mack, J., and Bolton, J. R.: Photochemistry of nitrite and nitrate in aqueous solution: a review, J. Photochem. Photobio. A, 128, 1-13, https://doi.org/10.1016/S1010-6030(99)00155-0, 1999.

Mark, G., Korth, H.G., Schuchmann, H.P., and von Sonntag, C.: The photochemistry of aqueous nitrate ion revisited, J. Photochem. Photobio. A, 101, 89-103, https://doi.org/10.1016/S1010-6030(96)04391-2, 1996.

Mozurkewich, M.: Mechanisms for the release of halogens from sea-salt particles by free radical reactions, J. Geophys. Res, 100, 14199-14207, http://dx.doi.org/10.1029/94JD00358, 1995.

Niu, J., Li, Y., and Wang, W.: Light-source-dependent role of nitrate and humic acid in tetracycline photolysis: kinetics and mechanism, Chemosphere, 92, 1423-1429, http://dx.doi.org/10.1016/j.chemosphere.2013.03.049, 2013.

Quan, J., Liu, Q., Li, X., Gao, Y., Jia, X., Sheng, J., and Liu, Y.: Effect of heterogeneous aqueous reactions on the secondary formation of inorganic aerosols during haze events, Atmos. Environ, 122, 306-312, http://dx.doi.org/10.1016/j.atmosenv.2015.09.068, 2015.

Richards-Henderson, N. K., Callahan, K. M., Nissenson, P., Nishino, N., Tobias, D. J., and Finlayson-Pitts, B. J.: Production of gas phase NO_2 and halogens from the photolysis of thin water films containing nitrate, chloride and bromide ions at room temperature, Phys. Chem. Chem. Phys, 15, 17636-17646, http://dx.doi.org/10.1039/C3CP52956H, 2013.

Richards, N. K., Wingen, L. M., Callahan, K. M., Nishino, N., Kleinman, M. T., Tobias, D. J., and Finlayson-Pitts, B. J.: Nitrate ion photolysis in thin water films in the presence of bromide ions, J. Phys. Chem. A, 115, 5810-5821, http://dx.doi.org/10.1021/jp109560j, 2011.

Richards, N. K., and Finlayson-Pitts, B. J.: Production of gas phase NO_2 and halogens from the photochemical oxidation of aqueous mixtures of sea salt and nitrate ions at room temperature, Environ. Sci. Technol, 46, 10447-10454, http://dx.doi.org/10.1021/es300607c, 2012.

Scharko, N. K., Berke, A. E., and Raff, J. D.: Release of nitrous acid and nitrogen dioxide from nitrate photolysis in acidic aqueous solutions, Environ. Sci. Technol, 48, 11991-12001, http://dx.doi.org/10.1021/es503088x, 2014.

Seinfeld, J., and Pandis, S.: Atmospheric chemistry and physics: from air pollution to climate change, John. Wiley. Sons, New York, 2006.

Shen, X., Lee, T., Guo, J., Wang, X., Li, P., Xu, P., Wang, Y., Ren, Y., Wang, W., Wang, T., Li, Y., Carn, S. A., and Collett, J. L.: Aqueous phase sulfate production in clouds in eastern China, Atmos. Environ, 62, 502-511, https://doi.org/10.1016/j.atmosenv.2012.07.079, 2012.

Shuali, U., Ottolenghi, M., Rabani, J., and Yelin, Z.: Photochemistry of aqueous nitrate solutions excited in the 195-nm band, J. Phys. Chem, 73, 3445-3451, https://doi.org/10.1021/j100844a052, 1969.

Sun, Y., Jiang, Q., Wang, Z., Fu, P., Li, J., Yang, T., and Yin, Y.: Investigation of the sources and evolution processes of severe haze pollution in Beijing in January 2013, J. Geophys. Res. Atmos, 119, 4380-4398, https://doi.org/10.1002/2014JD021641, 2014.

Sun, Y. L., Wang, Z. F., Fu, P. Q., Yang, T., Jiang, Q., Dong, H. B., Li, J., and Jia, J. J.: Aerosol composition, sources and processes during wintertime in Beijing, China, Atmos. Chem. Phys., 13, 4577-4592, https://doi.org/10.5194/acp-13-4577-2013, 2013.

Tan, Z., Rohrer, F., Lu, K., Ma, X., Bohn, B., Broch, S., Dong, H., Fuchs, H., Gkatzelis, G. I., Hofzumahaus, A., Holland, F., Li, X., Liu, Y., Liu, Y. H., Novelli, A., Shao, M., Wang, H. C., Wu, Y. S., Zeng, L. M., H, M., Kiendler-Scharr, A., Wahner, A., and Zhang, Y. H.: Wintertime photochemistry in Beijing: observations of RO_x radical concentrations in the North China Plain during the BEST-ONE campaign, Atmos. Chem. Phys., 18, 12391-12411, https://doi.org/10.5194/acp-18-12391-2018, 2018.

Tao, J., Zhang, Z., Tan, H., Zhang, L., Wu, Y., Sun, J., Che, H., Cao, J., Cheng, P., Chen, L., and Zhang, R.: Observational evidence of cloud processes contributing to daytime elevated nitrate in an urban atmosphere, Atmos. Environ, 186, 209-215, https://doi.org/10.1016/j.atmosenv.2018.05.040, 2018.

Tong, S. Y., Kong, L. D., Yang, K. J., Shen, J. D., Chen, L., Jin, S. Y., Wang, C., Sha, F., Wang, L.: Characteristics of air pollution episodes influenced by biomass burning pollution in Shanghai, China, Atmos. Environ, 117756, https://doi.org/10.1016/j.atmosenv.2020.117756, 2020.

Troian-Gautier, L., Turlington, M. D., Wehlin, S. A. M., Maurer, A. B., Brady, M. D., Swords, W. B., and Meyer, G. J.: Halide photoredox chemistry, Chem. Rev, 119, 4628-4683, https://doi.org/10.1021/acs.chemrev.8b00732, 2019.

Turnipseed, A. A., Vaghjiani, G. L., Thompson, J. E., and Ravishankara, A. R.: Photodissociation of HNO_3 at 193, 222, and 248 nm: Products and quantum yields, J. Chem. Phys, 96, 5887-5895, https://doi.org/10.1063/1.462685, 1992.

Vogt, R., Crutzen, P. J., and Sander, R.: A mechanism for halogen release from sea-salt aerosol in the remote marine boundary layer, Nature, 383, 327, http://dx.doi.org/10.1038/383327a0, 1996.

Wagner, I., Strehlow, H., and Busse, G.: Flash photolysis of nitrate ions in aqueous solution, J. Chem. Soc. A, 123, 1-33, http://dx.doi.org/10.1524/zpch.1980.123.1.001, 1980.

Wang, G., Zhang, R., Gomez, M. E., Yang, L., Zamora, M. L., Hu, M., Lin, Y., Peng, J., Guo, S., Meng, J., Li, J., Cheng, C., Hu, T., Ren, Y., Wang, Y., Gao, J., Cao, J., An, Z., Zhou, W., Li, G., Wang, J., Tian, P., Marrero-Ortiz, W., Secrest, J., Du, Z., Zheng, J., Shang, D., Zeng, L., Shao, M., Wang, W., Huang, Y., Wang, Y., Zhu, Y., Li, Y., Hu, J., Pan, B., Cai, L., Cheng, Y., Ji, Y., Zhang, F., Rosenfeld, D., Liss, P. S., Duce, R. A., Kolb, C. E., Molina. M. J.: Persistent sulfate formation from London fog to Chinese haze, Proc. Natl. Acad. Sci. USA, 113, 13630–13635, http://dx.doi.org/10.1073/pnas.1616540113, 2016.

Wingen, L. M., Moskun, A. C., Johnson, S. N., Thomas, J. L., Roeselova, M., Tobias, D. J., Kleinman, M. T., and Finlayson-Pitts, B. J.: Enhanced surface photochemistry in chloride-nitrate ion mixtures, Phys. Chem. Chem. Phys, 10, 5668-5677, http://dx.doi.org/10.1039/b806613b, 2008.

Xia, S.S., Eugene, A. J., and Guzman, M. I.: Cross photoreaction of glyoxylic and pyruvic acids in model aqueous aerosol, J. Phys. Chem. A, 122, 6457-6466, http://dx.doi.org/10.1021/acs.jpca.8b05724, 2018.

Xu, W., Kuang, Y., Zhao, C., Tao, J., Zhao, G., Bian, Y., Yang, W., Yu, Y., Shen, C., Liang, L., Zhang, G., Lin, W., and Xu, X.: NH_3-promoted hydrolysis of NO_2 induces explosive growth in HONO, Atmos. Chem. Phys, 19, 10557-10570, http://dx.doi.org/10.5194/acp-19-10557-2019, 2019.

Yabushita, A., Iida, D., Hama, T., and Kawasaki, M.: Direct observation of OH radicals ejected from water ice surface in the photoirradiation of nitrate adsorbed on ice at 100 K, J. Phys. Chem. A, 112, 9763-9766, http://dx.doi.org/10.1021/jp804622z, 2008.

Ye, C., Gao, H., Zhang, N., and Zhou, X.: Photolysis of nitric acid and nitrate on natural and artificial surfaces, Environ. Sci. Technol, 50, 3530-3536, http://dx.doi.org/10.1021/acs.est.5b05032, 2016.

Ye, C., Liu, P., Ma, Z., Xue, C., Zhang, C., Zhang, Y., Liu, J., Liu, C., Sun, X., and Mu, Y.: High H_2O_2 concentrations observed during haze periods during the winter in Beijing: Importance of H_2O_2 oxidation in sulfate formation, Environ. Sci. Technol. Lett, 5, 757-763, http://dx.doi.org/10.1021/acs.estlett.8b00579, 2018.

Zhang, K., and Parker, K. M.: Halogen radical oxidants in natural and engineered aquatic systems, Environ. Sci. Technol, 52, 9579-9594, http://dx.doi.org/10.1021/acs.est.8b02219, 2018.

Zheng, B., Zhang, Q., Zhang, Y., He, K. B., Wang, K., Zheng, G. J., Duan, F. K., Ma, Y. L., and Kimoto, T.: Heterogeneous chemistry: a mechanism missing in current models to explain secondary inorganic aerosol formation during the January 2013 haze episode in North China, Atmos. Chem. Phys, 14, 2031-2049, http://dx.doi.org/10.5194/acp-15-2031-2015, 2015a.

Zheng, G., K. Duan, F., Su, H., L. Ma, Y., Cheng, Y., Zheng, B., Zhang, Q., Huang, T., Kimoto, T., Chang, D., Pöschl, U., Cheng, Y., and B. He, K.: Exploring the severe winter haze in Beijing: The impact of synoptic weather, regional transport and heterogeneous reactions, Atmos. Chem. Phys, 15, 2969-

https://doi.org/10.5194/acp-2020-806
Preprint. Discussion started: 31 August 2020

2983, http://dx.doi.org/10.5194/acp-15-2969-2015, 2015b.

Figure Captions

Figure 1. Sulfate formation in the presence and absence of nitrate photolysis and O_2 under (a) solar irradiation and (b) 313 nm UV light. The concentrations of $NaHSO_3$ and the added NH_4NO_3 were both 30 mM. The light intensity was 8 mW/cm^2.

Figure 2. Generation of NO_x during nitrate photolysis under 313 nm UV light.

Figure 3. Sulfate formation at different pH values adjusted by the addition of $(NH_4)_2SO_4$ (AS), NH_4HSO_4 (ABS) and the mixture of $(NH_4)_2SO_4$ and NH_4HSO_4, respectively. Reaction conditions: 30 mM $NaHSO_3$, 30 mM NH_4NO_3, light (8 mW/cm^2) and air.

Figure 4. Comparison of NH_4NO_3 and $NaNO_3$ as the source of NO_3^- for sulfate formation at different pH. Reaction conditions: 30 mM $NaHSO_3$, 30 mM NH_4NO_3 or $NaNO_3$, light (8 mW/cm^2) and air.

Figure 5. Inhibition of 2-propanol on aqueous phase oxidation of bisulfite. Reaction conditions: 30 mM $NaHSO_3$, 30 mM NH_4NO_3, 20 mM 2-propanol, light (8 mW/cm^2) and air.

Figure 6. H_2O_2 produced during the photochemical reaction of nitrate under 313nm irradiation.

Figure 7. (a) Effects of halide ions on aqueous phase oxidation of bisulfite under light and (b) comparison of the effects of halide ions under dark and light conditions. Reaction conditions: 30 mM $NaHSO_3$, 30 mM NH_4NO_3, 30 mM NaCl, NaBr and NaI, respectively, light (8 mW/cm^2) and air.

Tables

Table 1. •OH quantum yields of nitrate photolysis as a function of pH.

Table 2. Reactions and their rate constants or quantum yields involved in this study.

https://doi.org/10.5194/acp-2020-806
Preprint. Discussion started: 31 August 2020

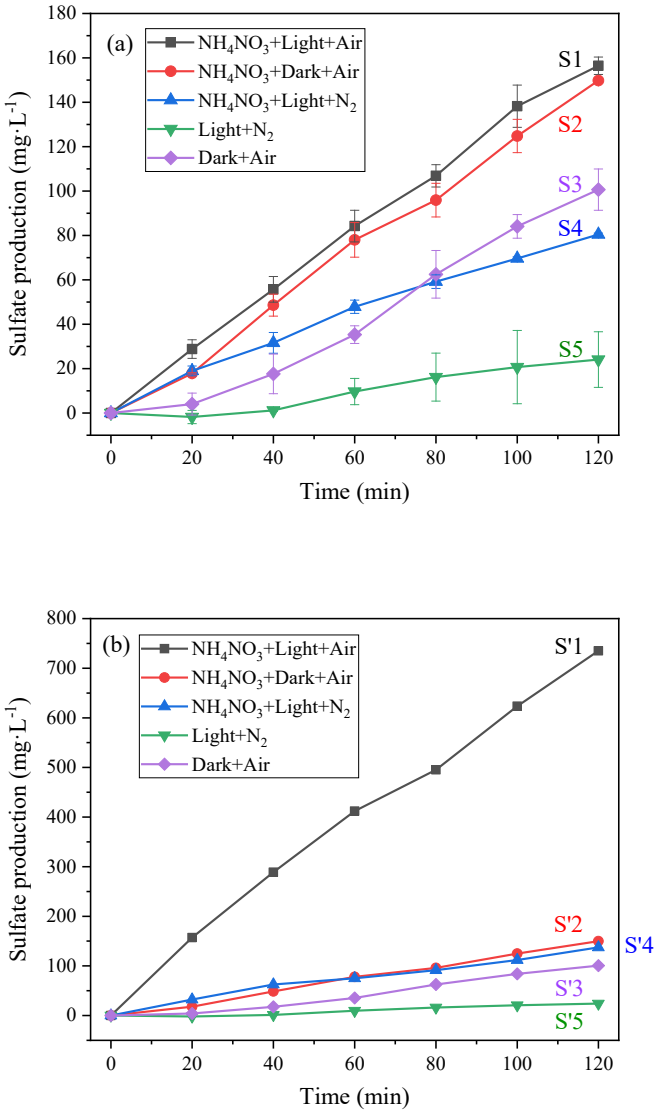

Figure 1. Sulfate formation in the presence and absence of nitrate photolysis and O_2 under (a) solar irradiation and (b) 313 nm UV light. The concentrations of $NaHSO_3$ and the added NH_4NO_3 were both 30 mM. The light intensity was 8 mW/cm^2.

https://doi.org/10.5194/acp-2020-806
Preprint. Discussion started: 31 August 2020

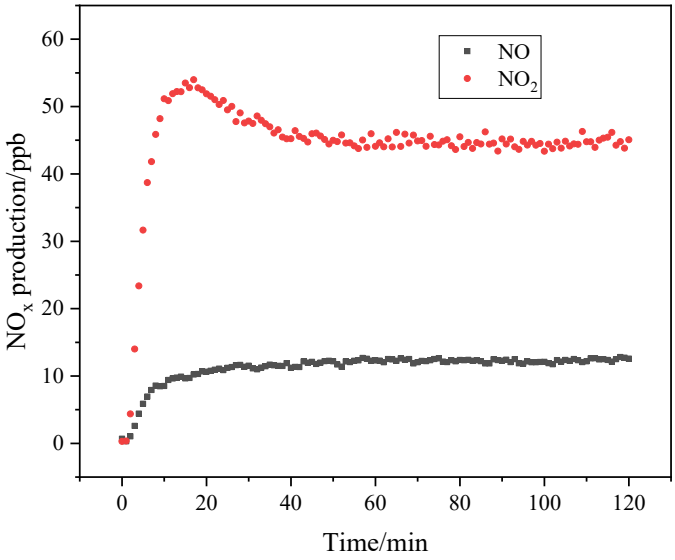

Figure 2. Generation of NO_x during nitrate photolysis under 313 nm UV light.

https://doi.org/10.5194/acp-2020-806
Preprint. Discussion started: 31 August 2020

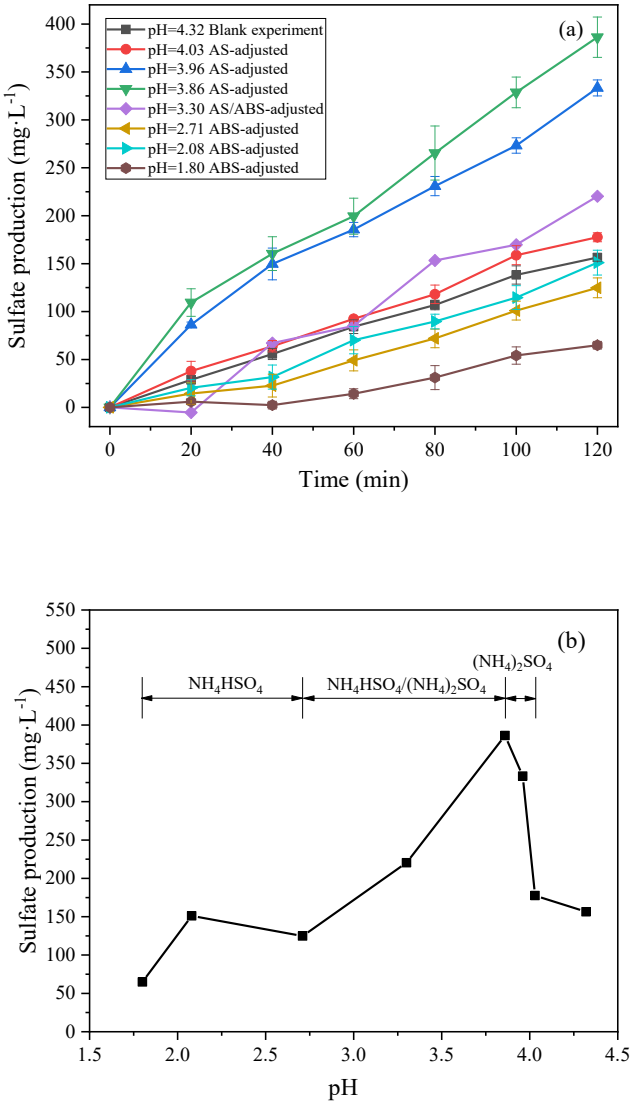

Figure 3. Sulfate formation at different pH values adjusted by the addition of $(NH_4)_2SO_4$ (AS), NH_4HSO_4 (ABS) and the mixture of $(NH_4)_2SO_4$ and NH_4HSO_4, respectively. Reaction conditions: 30 mM $NaHSO_3$, 30 mM NH_4NO_3, light (8 mW/cm^2) and air.

https://doi.org/10.5194/acp-2020-806
Preprint. Discussion started: 31 August 2020

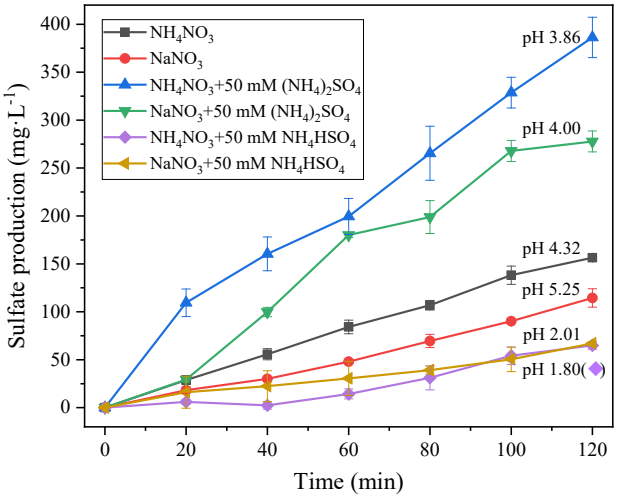

Figure 4. Comparison of NH_4NO_3 and $NaNO_3$ as the source of NO_3^- for sulfate formation at different pH. Reaction conditions: 30 mM $NaHSO_3$, 30 mM NH_4NO_3 or $NaNO_3$, light (8 mW/cm^2) and air.

https://doi.org/10.5194/acp-2020-806
Preprint. Discussion started: 31 August 2020

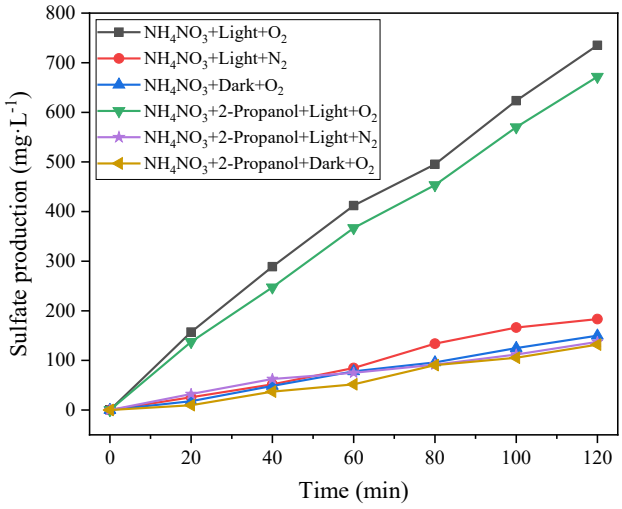

Figure 5. Inhibition of 2-propanol on aqueous phase oxidation of bisulfite under 313 nm irradiation. Reaction conditions: 30 mM $NaHSO_3$, 30 mM NH_4NO_3, 20 mM 2-propanol, light (8 mW/cm^2) and air.

https://doi.org/10.5194/acp-2020-806
Preprint. Discussion started: 31 August 2020

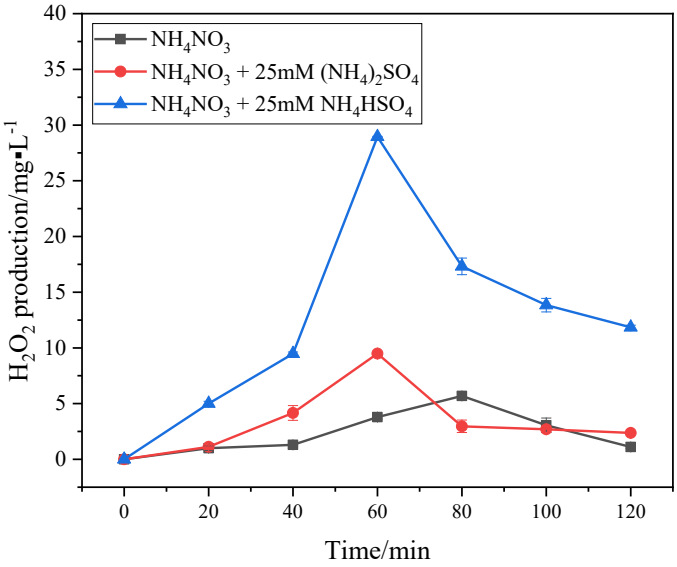

Figure 6. H_2O_2 produced during the photochemical reaction of nitrate under 313 nm irradiation.

https://doi.org/10.5194/acp-2020-806
Preprint. Discussion started: 31 August 2020

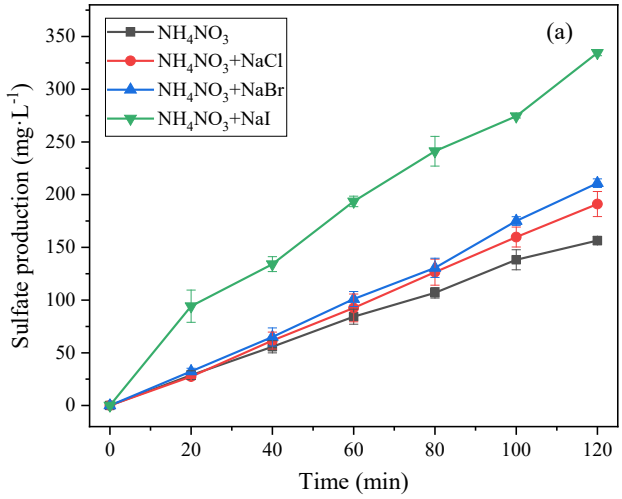

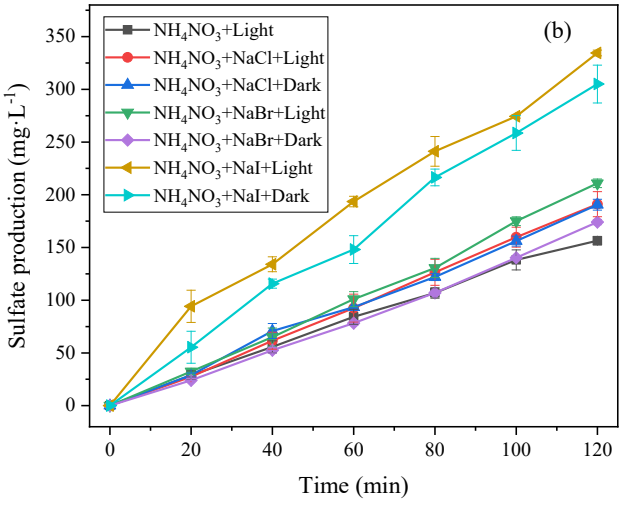

Figure 7. (a) Effects of halide ions on aqueous phase oxidation of bisulfite under light and (b) comparison of the effects of halide ions under dark and light conditions. Reaction conditions: 30 mM $NaHSO_3$, 30 mM NH_4NO_3, 30 mM NaCl, NaBr and NaI, respectively, light (8 mW/cm^2) and air.

https://doi.org/10.5194/acp-2020-806
Preprint. Discussion started: 31 August 2020

Table 1. •OH quantum yields of nitrate photolysis as a function of pH.

Conditions	pH	$\Phi_{\cdot OH}$ ($\times 10^{-3}$)
Air	4.32	4.240 ± 0.353
Air	4.03	4.033 ± 0.525
Air	3.96	7.785 ± 0.490
Air	2.71	8.252 ± 0.226
Air	2.08	16.672 ± 0.899

https://doi.org/10.5194/acp-2020-806
Preprint. Discussion started: 31 August 2020

Atmospheric Chemistry and Physics Discussions

Table 2. Reactions and their rate constants or quantum yields involved in this study.

No.	Reaction	*k* or Φ	Ref
R1	$SO_{2(g)} \overset{k_1}{\Leftrightarrow} SO_2{\cdot}H_2O \overset{k_2}{\Leftrightarrow} HSO_3^- + H^+ \overset{k_3}{\Leftrightarrow} SO_3^{2-} + 2H^+$	k_1=1.23; k_2=1.3×10^{-2}; k_3=6.6×10^{-8}	(Alexander et al., 2003;Gen et al., 2019b)
R2	$HSO_5^- + H_2O_2 \rightarrow HSO_4^- + H_2O$	k = 7.45×10^7 M^{-1} s^{-1}	(Seinfeld and Pandis, 2006;Ye et al., 2018;Shen et al., 2012)
R3	$NO_3^- + h\nu\ (+H^+) \rightarrow NO_2 + {\cdot}OH$	k=8.5×10^{-7} s^{-1}; Φ (λ=305 nm) = (9.2±0.4) × 10^{-3}	(Scharko et al., 2014;Yabushita et al., 2008)
R4	$NO_3^- + h\nu \rightarrow NO_2 + O^-$	Φ (λ > 290 nm) = 0.01	(Scharko et al., 2014)
R5	$NO_3^- + h\nu \rightarrow NO_2^- + O(^3P)$	k =8.5×10^{-8} s^{-1}; Φ (λ=305 nm) = 0.001	(Scharko et al., 2014)
R6	$2NO_2 + H_2O \rightarrow HONO + H^+ + NO_3^-$	k = 1×10^8	(Li et al., 2018b;Richards-Henderson et al., 2013)
R7	$2NO_2 + H_2O + h\nu \rightarrow HONO + {\cdot}OH$	k = 1.7×10^{-10} cm^3 mol^{-1} s^{-1}	(Bao et al., 2018;Gligorovski et al., 2015)
R8	$NO_2^- + H_2O \rightarrow HONO + OH^-$	—	(Yabushita et al., 2008)
R9	$O^- + H^+ / H_3O^+ \rightarrow {\cdot}OH + H_2O$	—	(Yabushita et al., 2008)
R10	$HONO(\text{or } NO_2^- + H^+) + h\nu \rightarrow {\cdot}OH + {\cdot}NO$	k =1.0×10^{-3} s^{-1}; Φ (λ< 390 nm) = 1.0	(Li et al., 2018b;Scharko et al., 2014)
R11	$NO_2 + HSO_3^- + H_2O \rightarrow 3H^+ + 2NO_2^- + SO_4^{2-}$	—	(Clifton et al., 1988)
R12	$NO_2 + HSO_3^- + H_2O + O_2 \rightarrow H^+ + NO_3^- + {\cdot}OH + HSO_4^-$	—	(Li et al., 2018b)
R13	$NO_2 + h\nu \rightarrow NO + O$	k = 1.1×10^{-2} s^{-1}	(Scharko et al., 2014)
R14	$HONO + h\nu \rightarrow NO + OH$	k = 1.0×10^{-3} s^{-1}	(Scharko et al., 2014)
R15	${\cdot}OH + H_2O_2 \rightarrow H_2O + {\cdot}HO_2$	k = 2.7×10^7 M^{-1} s^{-1}	(Hislop and Bolton, 1999;Gligorovski et al., 2015)
R16	$O(^3P) + O_2 \rightarrow O_3$	k = 4×10^9 M^{-1} s^{-1}	(Dubowski et al., 2001;Herrmann, 2007)
R17	$X^- + h\nu \rightarrow X^{\bullet} + e^-$	—	(Zhang and Parker, 2018)
R18	$X^{\bullet} + X^-$ (or Y^-) $\rightleftharpoons X_2^{\bullet -}$ (or $XY^{\bullet -}$)	k =8.5×10^9(Cl)/1.6-2.8×10^9(Br)/0.1-1.2×10^{10}(I) M^{-1} s^{-1}	(Zhang and Parker, 2018;Troian-Gautier et al., 2019)
R19	$^{\bullet}OH + X^- \rightleftharpoons HOX^{\bullet -} \rightleftharpoons OH^- + X^{\bullet}$	—	(Zhang and Parker, 2018)

https://doi.org/10.5194/acp-2020-806
Preprint. Discussion started: 31 August 2020

Table 2. Reactions and their rate constants or quantum yields involved in this study (continued).

No.	Reaction	*k* or Φ	Ref
R20	$HOX^{\bullet-} + H^+ \rightleftharpoons H_2O + X^\bullet$	—	(Zhang and Parker, 2018)
R21	$HOX^{\bullet-} + X^-$ (or Y^-) $\rightleftharpoons OH^- + X_2^{\bullet-}$ (or $XY^{\bullet-}$)	—	(Zhang and Parker, 2018)
R22	$SO_4^{\bullet-} + X^- \rightarrow SO_4^{2-} + X^\bullet$	—	(Zhang and Parker, 2018)
R23	$HSO_5^- + Br^- \rightarrow SO_4^{2-} + HOBr$	—	(Mozurkewich, 1995)
R24	$HOX + h\nu \rightarrow X^\bullet + {}^\bullet OH$	—	(Zhang and Parker, 2018)
R25	$X^\bullet + X^\bullet$ (or $Y^\bullet$) $\rightarrow X_2$ (or XY)	—	(Zhang and Parker, 2018)
R26	$X^\bullet + X_2^{\bullet-} \rightarrow X_2 + X^-$	—	(Zhang and Parker, 2018)
R27	$X_2^{\bullet-} + X_2^{\bullet-} \rightarrow X_3^- + X^-$ (or $X_2 + 2X^-$)	k =1.9-9×10^9(Cl)/0.9-1.2×10^{10}(Br)/3.2-3.9×10^{10}(I) M^{-1} s^{-1}	(Zhang and Parker, 2018;Troian-Gautier et al., 2019)
R28	$X^\bullet + {}^\bullet OH \rightarrow HOX$	—	(Zhang and Parker, 2018)
R29	$X_2^{\bullet-} + {}^\bullet OH \rightarrow HOX + X^-$	—	(Zhang and Parker, 2018)
R30	$HOBr + Br^- + H^+ \rightarrow Br_2 + H_2O$	k =1.6×10^{10} L mol^{-1} s^{-1}	(Richards-Henderson et al., 2013;Mozurkewich, 1995)
R31	$HOBr + Cl^- + H^+ \rightarrow BrCl + H_2O$	2.3 × 10^{10} M^{-2} s^{-2}	(Richards and Finlayson-Pitts, 2012;Vogt et al., 1996)
R32	$2{}^\bullet OH + 2Cl^- \rightarrow Cl_2 + 2OH^-$	—	(Alexander et al., 2003)
R33	$2{}^\bullet OH + 2Br^- \rightarrow Br_2 + 2OH^-$	—	(Richards-Henderson et al., 2013)
R34	$2{}^\bullet OH + Br^- + Cl^- \rightarrow BrCl + 2OH^-$	—	(Richards and Finlayson-Pitts, 2012)
R35	$NO_3^- + 3H^+ + 2Br^- \rightarrow Br_2 + HONO + H_2O$	—	(Richards-Henderson et al., 2013)
R36	$HSO_3^- + HOX \rightarrow 2H^+ + X^- + SO_4^{2-}$	—	this work
R37	$HSO_3^- + X_2 + H_2O \rightarrow 3H^+ + 2X^- + SO_4^{2-}$	—	this work
R38	$HSO_3^- + HOCl \rightarrow SO_4^- + 2H^+ + Cl^-$	—	(Vogt et al., 1996)
R39	$HSO_3^- + HOBr \rightarrow SO_4^- + 2H^+ + Br^-$	—	(Vogt et al., 1996)